

3658

Evidence for Mesoscale Gaussian Water Diffusion in Living Human Brain

Kulam Najmudeen Magdoom^{1,2}, Alexandru V Avram¹, Thomas E. Witzel³, Susie Yi Huang³, and Peter J Basser¹¹National Institutes of Health, Bethesda, MD, United States, ²The Military Traumatic Brain Injury Initiative (MTBI2), The Henry M Jackson Foundation for the Advancement of Military Medicine (HJF) Inc., Bethesda, MD, United States, ³Athinoula A. Martinos Center for Biomedical Imaging, Massachusetts General Hospital, Boston, MA, United States

Synopsis

Keywords: Microstructure, Brain

Motivation: Diffusion MRI is a promising means to map mesoscopic human brain architecture *in vivo*, however an appropriate model is required that relates the MR signal and features of the underlying microstructure within the voxel.

Goal(s): The goal of this study is to determine whether a Gaussian diffusion model is applicable at the mesoscale.

Approach: We compared single and double diffusion encoded signals acquired with large b-values at two different diffusion times to test for Gaussianity.

Results: We found no significant time-dependence in the diffusion weighted signals in brain parenchyma, confirming the applicability of the Gaussian diffusion at the mesoscale.

Impact: The study resolves the ongoing debate on the appropriate model to use to analyze the diffusion weighted signals in live human brain at clinically accessible spatiotemporal scales.

Introduction

Imaging brain tissues properties at the mesoscopic scale provides invaluable information to study normal and abnormal brain development and function. Diffusion tensor distribution (DTD) MRI continues to be attractive for elucidating mesoscopic tissue architecture by modeling the voxel as composed of an ensemble of mesoscopic water pools undergoing Gaussian diffusion [1-3]. The validity of this assumption for the live human brain at clinically accessible spatiotemporal scales is still unclear. In this study, we acquired single and double diffusion encoded (SDE, DDE) signals from human brains *in vivo* at two different diffusion times while fixing all other MRI parameters to test for time dependence of the signal and resulting DTD MRI derived measures.

Methods

Diffusion weighted signals were acquired using a novel double PFG pulse sequence called interfused-PFG, (iPFG), [3] with EPI readout and multi-band (MB) slice excitation (Figure 1), which uses efficient trapezoidal gradients with well-defined diffusion times. Diffusion encoding was obtained using rank-1 and rank-2 b-tensors also depicted in Figure 1. The two independent gradients in the diffusion block were estimated numerically to yield a set of 216 diffusion encoding b-tensors with uniform distribution of sizes ($b = 0 - 5,000 \text{ s/mm}^2$), shapes, and orientations for unbiased estimation of the DTD.

DW signals were used to estimate the DTD at the two bracketing diffusion times using methods outlined in [3]. We assume the DTD to be the maximum entropy normal tensor variate distribution (NTVD) [4] with samples constrained to be positive definite (CNTVD) to ensure physicality [2,5]. The estimated DTD was used to synthesize micro-diffusion tensors within each voxel whose corresponding ellipsoids' size, shape and orientation heterogeneity were quantified using measures derived from their eigenvalue and eigenvector distributions.

MRI data was acquired in 40% polyvinylpyrrolidone (PVP) phantom for control, and five healthy young adults on a 3T scanner (MAGNETOM Connectome, Siemens Healthineers) with 300 mT/m peak gradient strength and a 200 T/m/s slew rate using 64-channel coil. Whole-brain DTD MRI data was acquired using the following parameters: $\tau = 11\backslash37,74 \text{ ms}$, $\text{FOV} = 192 \times 192 \times 140 \text{ mm}$, MB factor = 3, GRAPPA acceleration factor = 2, $\text{TR/TE} = 4,600\backslash145 \text{ ms}$, and a 2 mm isotropic spatial resolution. For comparison, the images from the two diffusion times were registered with the non-diffusion weighted volume using FSL [6].

Results and Discussion

A representative set of four b-tensors was chosen for raw DWIs which includes both rank-1 and rank-2 with small, medium, and large b-values. The absolute difference between the DWIs acquired at both diffusion times and the distribution of their intensities are also shown to delineate the differences in the signal between the two diffusion times. The DTI and DTD measures were mapped for the brain using the data acquired.

The DWIs acquired on PVP phantom from the two diffusion times were nearly identical as shown by the absolute difference maps in the third row in Figure 2. There were small differences (< 3%) observed at the lower b-values which were manifest in non-zero shifts observed in the histogram of the signal differences, which could be due to coherence artifacts resulting from the long relaxation times of liquids compared to brain tissue.

The signal contrast in brain parenchyma for all b-tensors was very similar across diffusion times as verified by the white noise appearance of the absolute difference maps except at low b-values in Figure 3. This includes white matter regions such as corpus callosum and internal capsule where water is usually assumed to be restricted. At low b-values, larger signal differences were noted in CSF-filled regions likely due to pulsatile flow. The DTI and DTD measures for both diffusion times are shown in Figure 4. Given the similar signal trends, the maps of the model measures were indistinguishable and had expected values. The DWI differences across subjects for the two diffusion times are shown in Figure 5 with identical findings as shown for Figure 3.

Conclusion

Our *in vivo* human brain experiments revealed no significant measurable differences between the MDE or mPFG signal attenuation over a practical clinical range of diffusion times (37 - 74 ms). These results support the argument that over this range of diffusion times in living brain tissue, the Gaussian diffusion assumption/approximation holds for multiple mesoscopic water pools simultaneously. Our findings support the assumption that diffusion in brain tissue can be modeled using a mixture of Gaussian processes, which is a fundamental assumption of DTD estimation, but which was not previously validated. Thus, our findings justify the use of DTD-MRI for clinical applications over the broad range of diffusion times we investigated.

Acknowledgements

This study was supported by the Intramural Research Program of the NICHD. This work was partly funded by NIH BRAINInitiative grant 1U01EB026996-01 - "Connectome 2.0: Developing the next generation human MRI scanner for bridging studies of the micro-, meso- and macro-connectome.", and by the Department of Defense in the Military Traumatic Brain Injury Initiative under award, HU0001-22-2-0058. This work utilized computational resources of the NIH HPC Biowulf cluster (<http://hpc.nih.gov>). The authors have no conflicts of interest to disclose. The views, information or content, and conclusions presented do not necessarily represent the official position or policy of, nor should any official endorsement be inferred on the part of, the Uniformed Services University, the Department of Defense, the U.S. Government or the Henry M. Jackson Foundation for the Advancement of Military Medicine, Inc.

References

- Jian, B., Vemuri, B. C., Ozarslan, E., Carney, P. R. & Mareci, T. H. A novel tensor distribution model for the diffusion-weighted MR signal. *Neuroimage* 37, 164–76 (2007).
- Westin, Carl-Fredrik, et al. "Q-space trajectory imaging for multidimensional diffusion MRI of the human brain." *Neuroimage* 135 (2016): 345-362
- Magdoom, Kulam Najmudeen, et al. "A novel framework for in-vivo diffusion tensor distribution MRI of the human brain." *NeuroImage* 271 (2023): 120003
- Basser, Peter J., and Sinisa Pajevic. "A normal distribution for tensor-valued random variables: applications to diffusion tensor MRI." *IEEE transactions on medical imaging* 22.7 (2003): 785-794
- Magdoom, K. N., Pajevic, S., Dario, G., & Basser, P. J. (2021). A new framework for MR diffusion tensor distribution. *Scientific Reports*, 11(1), 2766
- Jenkinson, M., Beckmann, C. F., Behrens, T. E. J., Woolrich, M. W. & Smith, S. M. FSL. *NeuroImage* 62, 782–790 (2012).

Figures

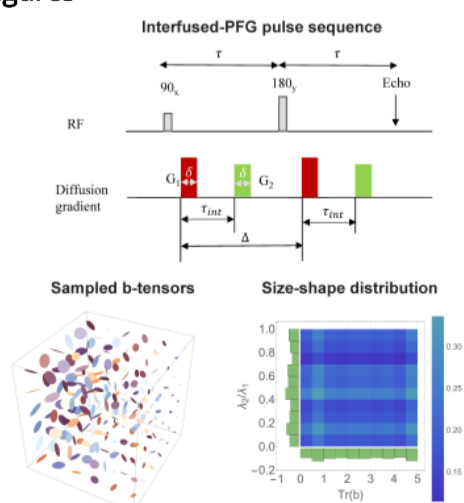


Figure 1: Interfused pulsed-field gradient (iPFG) sequence used to realize the rank-1 and rank-2 b-tensors that are displayed as sticks and ellipses, respectively. The parameters, G_1 and G_2 are the two independent diffusion gradient magnitudes, τ_{int} is the time between the two gradients (i.e., interfusing time), δ is the diffusion gradient duration, and Δ is the diffusion time. The uniform size-shape distribution of the b-tensors sampled at both diffusion times is displayed as a 2D histogram of $\text{trace}(b)$ and the ratio of non-zero eigenvalues of the b-tensor.

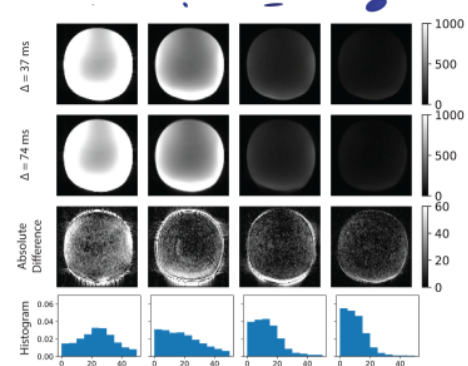


Figure 2: Multiple diffusion encoded (MDE) images of an axial slice of a PVP phantom acquired at two different diffusion times (i.e., $\Delta = 37/74$ ms). The rank-1/rank-2 b-tensors corresponding to each column are displayed as sticks and ellipses, respectively. The b-values of the plotted b-tensors are approximately 270, 1100, 3500, and 4820 s/mm^2 respectively. The absolute difference between the two images along with its histogram are shown in the third and fourth rows respectively.

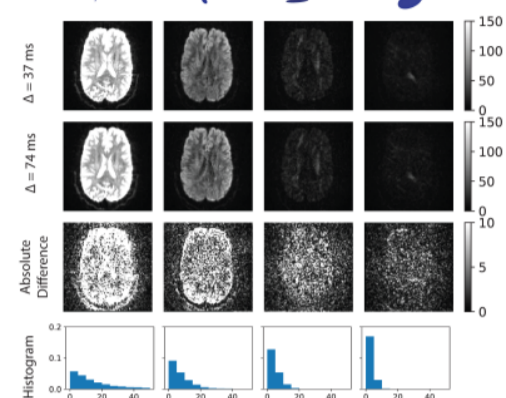


Figure 3: MDE images from an axial slice in the human brain of a representative subject acquired in vivo at two different diffusion times (i.e., $\Delta = 37/74$ ms). The rank-1/rank-2 b-tensors corresponding to each column are displayed as sticks and ellipses, respectively. The b-values of the plotted b-tensors are approximately 270, 1100, 3500, and 4820 s/mm^2 respectively. The absolute difference between the two images along with the corresponding histogram are shown in the third and fourth rows respectively.

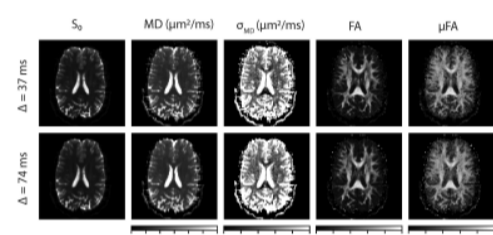


Figure 4: Microstructural measures derived from DTD MRI in an axial slice in the human brain acquired in vivo at two different diffusion times (i.e., $\Delta = 37/74$ ms). The measures include the non-diffusion weighted signal (S_0), mean diffusivity (MD), standard deviation of mean diffusivity (σ_{MD}), fractional anisotropy (FA) and microscopic fractional anisotropy (μFA). It can be observed that the value of the measures were as expected and nearly indistinguishable across the diffusion times tested.

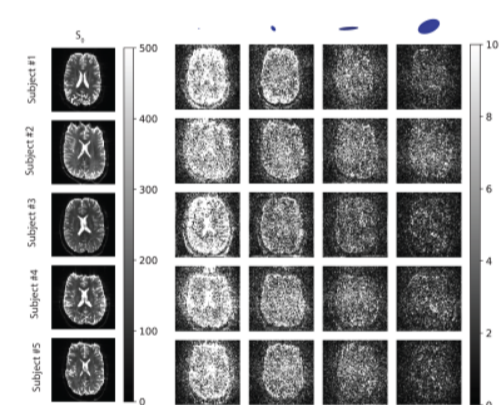


Figure 5: Absolute difference in MDE images relative to S_0 from an axial slice in the human brain of five healthy controls in vivo acquired at two different diffusion times (i.e., $\Delta = 37/74$ ms). The rank-1/rank-2 b-tensors corresponding to each column are displayed as sticks and ellipses, respectively. The b-values of the plotted b-tensors are approximately 270, 1100, 3500, and 4820 s/mm^2 respectively. The DWIs acquired with two diffusion times were nearly indistinguishable except at the lateral ventricles for all the subjects scanned.